AWARD NUMBER: W81XWH-16-1-0624

TITLE: Overcoming CRPC Treatment Resistance via Novel Dual AKR1C3 Targeting

PRINCIPAL INVESTIGATOR: Christopher P Evans MD

CONTRACTING ORGANIZATION: University of California, Davis

REPORT DATE: OCTOBER 2020

TYPE OF REPORT: ANNUAL

PREPARED FOR: U.S. Army Medical Research and Development Command
Fort Detrick, Maryland 21702-5012

DISTRIBUTION STATEMENT: Approved for Public Release;
Distribution Unlimited

The views, opinions and/or findings contained in this report are those of the author(s) and should not be construed as an official Department of the Army position, policy or decision unless so designated by other documentation.

REPORT DOCUMENTATION PAGE

Form Approved
OMB No. 0704-0188

Public reporting burden for this collection of information is estimated to average 1 hour per response, including the time for reviewing instructions, searching existing data sources, gathering and maintaining the data needed, and completing and reviewing this collection of information. Send comments regarding this burden estimate or any other aspect of this collection of information, including suggestions for reducing this burden to Department of Defense, Washington Headquarters Services, Directorate for Information Operations and Reports (0704-0188), 1215 Jefferson Davis Highway, Suite 1204, Arlington, VA 22202-4302. Respondents should be aware that notwithstanding any other provision of law, no person shall be subject to any penalty for failing to comply with a collection of information if it does not display a currently valid OMB control number. **PLEASE DO NOT RETURN YOUR FORM TO THE ABOVE ADDRESS.**

1. REPORT DATE	2. REPORT TYPE	3. DATES COVERED
OCTOBER 2020	ANNUAL	09/30/2019 – 09/29/2020

4. TITLE AND SUBTITLE
Overcoming CRPC Treatment Resistance via Novel Dual AKR1C3 Targeting

5a. CONTRACT NUMBER
W81XWH-16-1-0624

5b. GRANT NUMBER
PC150040P1

5c. PROGRAM ELEMENT NUMBER

6. AUTHOR(S)
Christopher P. Evans

E-Mail: cpevans@ucdavis.edu

5d. PROJECT NUMBER

5e. TASK NUMBER

5f. WORK UNIT NUMBER

7. PERFORMING ORGANIZATION NAME(S) AND ADDRESS(ES)

University of California, Davis
1850 Research Park Dr, Ste 300
Davis, CA 95618-6134

8. PERFORMING ORGANIZATION REPORT NUMBER

9. SPONSORING / MONITORING AGENCY NAME(S) AND ADDRESS(ES)

U.S. Army Medical Research and Development Command
Fort Detrick, Maryland 21702-5012

10. SPONSOR/MONITOR'S ACRONYM(S)

11. SPONSOR/MONITOR'S REPORT NUMBER(S)

12. DISTRIBUTION / AVAILABILITY STATEMENT
Approved for Public Release; Distribution Unlimited

13. SUPPLEMENTARY NOTES

14. ABSTRACT
Enzalutamide (Enza) and abiraterone (Abi) were approved for the treatment of metastatic castration resistant prostate cancer (mCRPC) patients. Resistance to Enza and Abi occurs frequently and renders mCRPC patients incurable. Therefore, there is great unmet medical need to identify resistant mechanisms to improve the treatment outcome of mCRPC. We have shown that overexpression of AKR1C3 is responsible for the elevated intracrine androgen biosynthesis in prostate cancer cells. Up-regulation of AKR1C3 is correlated with anti-androgen resistance. We therefore sought to knock down AKR1C3 with specific siRNA/shRNA and small molecule drug to confirm its role in androgen synthesis and drug resistance. We used siRNA, shRNA specific to AKR1C3 and a small molecule inhibitor Indomethacin to target AKR1C3. At cellular level, we demonstrated that knockdown AKR1C3 may: 1. Restore sensitivity to anti-androgen drugs such as enzalutamide and abiraterone. 2. Reduce AR-V7 level. 3. Inhibit AR transactivation activity. 4. Abate intratumoral androgen synthesis. Using Indocin to target AKR1C3 in vivo is efficient in reducing tumor sizes and further successful in blocking tumor growth when combined with either enzalutamide or abiraterone. Reduction of AR-V7 via AKR1C3 knockdown may also involves the regulation of hnRNAP1, the enzyme responsible for RNA splicing. Our results confirmed that blocking AKR1C3 restores drug sensitivity of CRPC or drug resistant cells to anti-androgen treatments. AKR1C3/AR-V7 axis also confers cross-resistance to apalutamide and darolutamide. Targeting AKR1C3 with Indomethacin in combination with anti-androgens such as enzalutamide shows great potential in advanced prostate cancer treatment.

15. SUBJECT TERMS
AKR1C3, intracrine androgens, enzalutamide, resistance

16. SECURITY CLASSIFICATION OF:			17. LIMITATION OF ABSTRACT	18. NUMBER OF PAGES	19a. NAME OF RESPONSIBLE PERSON
a. REPORT	b. ABSTRACT	c. THIS PAGE			USAMRMC
Unclassified	Unclassified	Unclassified	Unclassified	22	19b. TELEPHONE NUMBER *(include area code)*

Standard Form 298 (Rev. 8-98)
Prescribed by ANSI Std. Z39.18

TABLE OF CONTENTS

1. INTRODUCTION:

Aldo-keto reductase family 1 member C3 (AKR1C3), also named 17BHSD5, is one of the most important genes involved in androgen synthesis and metabolism. AKR1C3 facilitates the conversion of weak androgens androstenedione (A' dione) and 5 α- androstanedione (5α-dione) to the more active androgens, testosterone and DHT respectively, which cannot be inhibited by abiraterone. It catalyzes steroids conversion and modulates steroid receptors trans-activation. AKR1C3 is the major AKR1C isozyme expressed in the human prostate; and elevated expression of this enzyme has been associated with PCa progression and aggressiveness. We have demonstrated that AKR1C3 was up-regulation in anti-androgen resistant prostate cancer cells. This overexpression conferred resistance to enzalutamide and was reversible by either AKR1C3 inhibitor or RNA interference. Our hypothesis is that targeting AKR1C3 decreases intracrine androgens and AR variants and improves enzalutamide therapy against metastatic CRPC.

2. KEYWORDS:

Androgen synthesis pathways; tet-inducible AKR1C3 expression; steroid measurement by LC-MS analysis, Abiraterone resistance, orthotopic animal model

3. ACCOMPLISHMENTS:

In the beginning of the study, we first validated that **AKR1C3 affected intracrine androgen biosynthesis**. There are three known androgen metabolism pathways so far. In the classical pathway, cholesterols are converted into DHEA and then androstenedione, which then to testosterone by AKR1C3. In some studies showed that androstenedione is preferentially metabolized into 5'-dione, and then to dihydrotestosterone (DHT) by AKR1C3. The lately proposed backdoor pathway used for intracrine androgen synthesis suggests that steroid will be produced through androsterone and to androstenediol by AKR1C3 to reach DHT. AKR1C3 is essential in all three routes (**Figure 1**). Levels of AKR1C3 vary among prostate cancer cell lines. Two of the castration resistance prostate cancer (CRPC) lines, CWR22Rv1 and VCaP cells express high levels of endogenous AKR1C3; whereas LNCaP cells and the subline LNCaP C42B with low or sub-detectable levels.

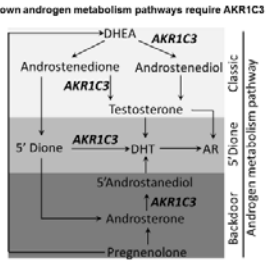

Figure 1. AKR1C3 is involved in the canonical, 5-diol, and backdoor pathways of androgen synthesis and activates AR.

Generation of tet-inducible AKR1C3 expression in LNCaP cells (led by Dr. Gao and assisted by Dr. Evans' labs) We therefore introduced constructs expressing AKR1C3 both alone or under the control of doxycycline into LNCaP cells, and selected for stable clones with respective antibiotics. Here we showed the characterization of the tet-inducible LNCaP/TR/AKR1C3 stale clone. With doxycycline in the dose of 1, 2.5 and 5 ng/ml treatments overnight, expression of AKR1C3 was induced in a dose-response manner (**Figure 2A**). At the same time, detection of AR-V7 and variants in general was apparent compared to the un-induced control. This observation is in agreement with our previous report that knocking down AKR1C3 in CWR22Rv1 and C4-2B-MDVR cells diminished AR-V7 expression. We further validated the biological function of the tet-inducible ARK1C3 in LNCaP/TR/AKR1C3 cells. When the gene was not induced, cell growth was readily inhibited by anti-androgens abiraterone (ABI) and enzalutamide (Enza). Addition of androgen synthesis intermediates for two of the pathways, 5α-dione or androstenedione bypassed the inhibition elicited by ABI (on CYP17A1) but not much by Enza, suggesting some leakiness of the tet-responsiveness. With doxycycline induction, the control treatment benefited from overexpression of AKR1C3 and partially overcame the ABI and Enza inhibition (**Figure 2B**). When using the straight AKR1C3 overexpresser LNCaP-AKR1C3, enhancement of transcriptional drive with the reporter construct PSA-Luc was vividly demonstrated by the same pair of pathway intermediates, androstenedione and 5α-dione (**Figure 3A and 3B**). PSA-Luc activities were driven by androstenedione and 5α-dione in LNCaP-AKR1C3 cells grown in charcoal stripped (CS) conditions. Line-up of LNCaP and C4-2B neo and AKR1C3 cells showed AKR1C3 overexpression and increase in AR variants (**Figure 3C**). LNCaP-AKR1C3 cells grown in CS medium were subjected ChIP assay and the result supported AR binding to its androgen response element (ARE) in AKR1C3 overexpressing LNCaP cells compared to the neo control in CS conditions (**Figure 3D**). Both transcript and protein levels of the AR surrogate marker, PSA, were significantly enhanced in LNCaP-AKR1C3 cells with *p* value less than 0.05 (**Figure 3E and 3F**).

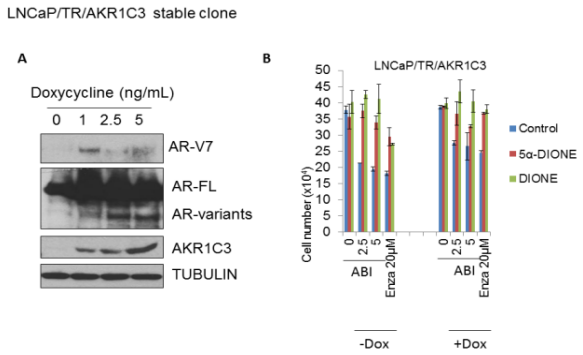

Figure 2. A. Validation of LNCaP/TR/AKR1C3 cells. B. Growth response of LNCaP/TR/AKR1C3 cells to stimuli of intermediates from androgen synthetic pathway.

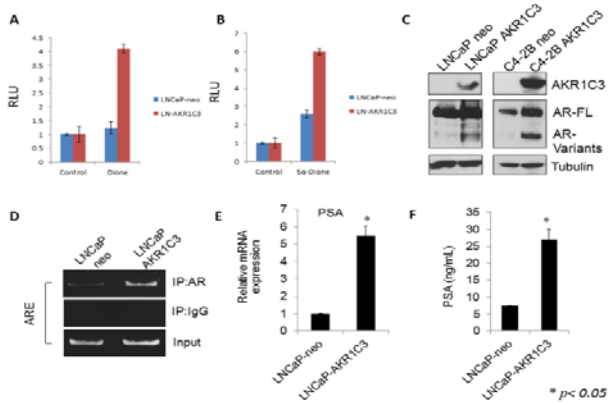

Figure 3. PSA-Luc assays for LNCaP-AKR1C3 cells with or without substrates androstenedion (A) or 5α-dione (B). C. Confirmation of AKR1C3 overexpression; D. ChIP assay for AR binding; and PSA measurements by q-PCR (E) and ELISA (F).

Measureing intracellular and intratumor androgen levels by LC-MS induced by AKR1C3 (led by Dr. Gao and assisted by Dr. Evans' labs)

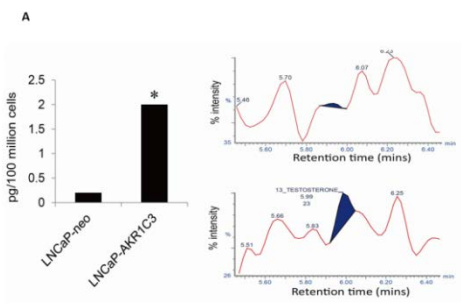

Metabolites (pg/100 million cells)	LNCaP-neo	LN-AKR1C3
Cholesterol	0.0	0.0
etiocholanolne glurcuronide	0.0	16.8
Coprostanol-7,12-diol	0.0	14834.3
27-OH-Cholesterol	14.5	67.4
24-Hydroxycholesterol	214.4	226.1
5a,6a-epoxycholesterol	0.0	57.3
Cholesterol-3-SO4	43955.4	68104.5
Taurocholanic acid	0.9	4.4
Cholesterol-3-Glu	103.8	172.3
Pregnenolone	0.0	0.0
Progesterone	6.5	24.1
20a-Hydroxy-5a-pregnan-3-one	0.0	49.3
17-OH-Pregnanolone-3-Glu-Na	0.0	173.1
Aldosterone	0.0	183.8
Androstenedione	0.0	0.0
Testosterone	0.2	2.1
Dihydrotestosterone	0	0
Etiocholanolone-3-Glu	0.0	288.4
Cortexone	0.0	0.0
Corticosterone	21.1	0.0

Figure 4. Steroids in LNCaP neo and AKR1C3 cells by LC-MS measurement. A. Testosterone; B. detailed lineups of various steroids detected in neo and AKR1C3 cells.

Due to the leakiness of the tet-inducible AKR1C3 line, we relied more on the LN-AKR1C3 and C4-2B-AKR1C3 cells to study the intracrine androgen biosynthesis and animal studies.

One hundred millions (1×10^8) of LNCaP neo and LNCaO-AKR1C3 cells were harvested before maintained in serum and phenol-red free medium for 3 days. Steroids were extracted from cell pellets with 50% methanol and the supernatants were lyophilized followed by subsequent reconstitution to lower the total volume for LC-MS analysis. LNCaP-AKR1C3 cells expressed a significant higher level of testosterone than the vector-control line (**Figure 4A**). The level of progesterone, an intermediate in the androgen biosynthesis pathway, was elevated by almost four fold in the AKR1C3 cells (**Figure 4B**). These results echoed with the enhanced PSA expression in LNCaP-AKR1C3 cells in **Figure 3E and 3F**. C4-2B AKR1C3 cells were harvested in the same fashion together with the neo cells for lysate collection subjected to the intracrine

Metabolites (pg/mg tissue)	C4-2B parental tumors	C4-2B MDVR tumors
Cholesterol	10626.1	14995.4
7-keto-25-OH cholesterol	493.8	637.4
Coprostanol-7,12-diol	0.0	0.0
27-OH-Cholesterol	0.0	1777.6
24-Hydroxycholesterol	660.9	9485.3
5a,6a-epoxycholesterol	8941.0	6803.1
Cholesterol-3-SO4	3500731.6	1695625.7
Taurocholanic acid	1163.2	1911.8
Cholesterol-3-Glu	7916.2	4293.3
5a-Dihydroprogesterone	883.2	974.7
20-Hydroxypregnenolone	2035.4	1035.3
20a-Hydroxy-5a-pregnan-3-one	3966.3	615.2
20a-Dihydroprogesterone	111.1	91.8
PREGNENOLONE	0.0	62.1
Progesterone	1005.7	1043.8
17-HYDROXYPROGESTERONE	58.5	22.0
TESTOSTERONE SULFATE	8.9	0.0
Testosterone GLUC	1218.3	343.5
Etiocholanolone-3-Glu	7551.9	7835.9
DHEAS	49.6	49.1
ALDOSTERONE	0.0	0.0
ANDROSTENEDIONE	194.7	142.7
TESTOSTERONE	1045.9	3458.6
ALLODIHYDROTESTOSTERONE	152.8	240.3
Estrone	295.0	452.5
ESTRADIOL	482.0	373.9
ESTRONE-SO4	42.4	58.9
ESTRONE GLU	0.0	159.4
4-OH ESTRONE	5842.9	15323.1
2-Methoxy-3 OH-estradiol	0.0	19.2
CORTEXONE	164.4	199.0
CORTICOSTERONE	19710.0	11398.3

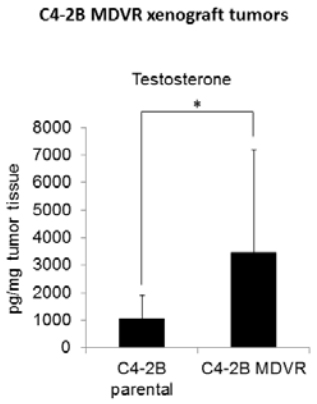

Figure 5. Detailed lineups of various steroids detected in C4-2B parental and MDVR cells by LC-MS measurement.

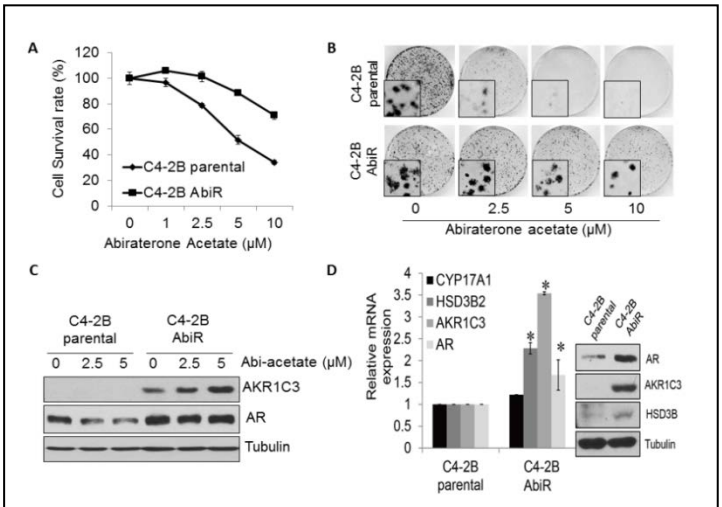

Figure 6. Cell survival curves (A) and clonogenic assays (B) of C4-2B parental and AbiR cells in response to various concentrations of Abi acetate; Characterization of C4-2B AbiR cells in the presence of Abi acetate (C) or in comparison with other lines (D); Examination of other steroidogenic enzymes in AbiR cells by qPCR and Western blotting.

androgen measurement by LC-MS analysis. The samples are currently processed in the West Coast Metabolic Center, UCD. However, we were inspired by the intracrine androgen data from xenograft tumors from C4-2B and C4-2B MDVR orthotopic models. The testosterone level in the MDVR tumors was 3 times higher than the parental one (**Figure 5**). Moreover, there was a significant change in the pregnenolone level. Being the immediate product after cholesterol in the steroidogenic pathway, pregnenolone is the main substrate for CYP17A1, target for Abi. We therefore characterized another drug resistant line from C4-2B cells, C4-2B AbiR cells.

C4-2B AbiR cells were resistant to Abi acetate in a dose-response manner compared to the parental line (**Figure 6A**). This result was also confirmed by the clonogenic assay (**Figure 6B**). Abi acetate significantly inhibited the number of colonies in C4-2B parental cells in a dose-dependent manner compared with C4-2B AbiR cells. C4-2B AbiR cells readily expressed increasing levels of AKR1C3 responding to Abi acetate treatments (**Figure 6C**). In addition of AR, variants and AKR1C3, some other steroidogenic enzymes such as CYP17A1 and HSD3B2 also displayed elevation in C4-2B AbiR cells in the mRNA and/or protein levels (**Figure 6D**). Testosterone level in C4-2B AbiR cell was 12 pg/50 million cells, similar to that in C4-2B MDVR or LNCaP-AKR1C3 cells. With the single drug resistant cell lines on hand, we tested for their cross-resistance to Enza and Abi. While the parental line was sensitive to both drugs, the resistant lines showed cross resistance to the other drug at an extent as depicted in both growth and clonogenic assays (**Figure 7A and 7B**). AR-V7 and variant levels in both MDVR and AbiR cells were detectable together with enhanced AR full-length and variants in general, when compared to those in the parental and LNCaP cells (**Figure 7C**). Knocking down AR-V7 with the specific siRNA resensitized both MDVR and AbiR cells to Abi (**Figure 7D**). To validate the role of AKR1C3 in regulating the leves of AR full-length and variants, we used two small hairpin RNA (shRNA) specific to AKR1C3 to knock down the expression. In C4-2B MDVR or known CRPC such as CWR22Rv1 and VCaP cells, shRNA #561 and

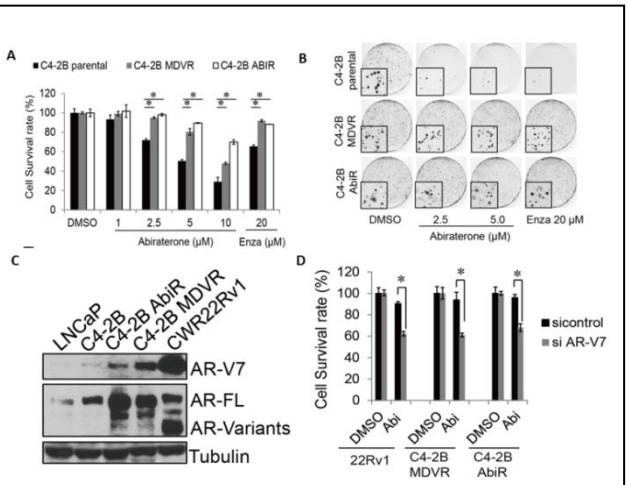

Figure 7. Cross-resistance of C4-2B MDVR and AbiR cells to Abi and Enza by growth (A) and clonogenic (B) assays. C. Levels of AR-V7 and variants in general were higher than the parental lines and similar to CWR22Rv1 cells D. Kinockdown of AR-V7 resensitized cells to Abi.

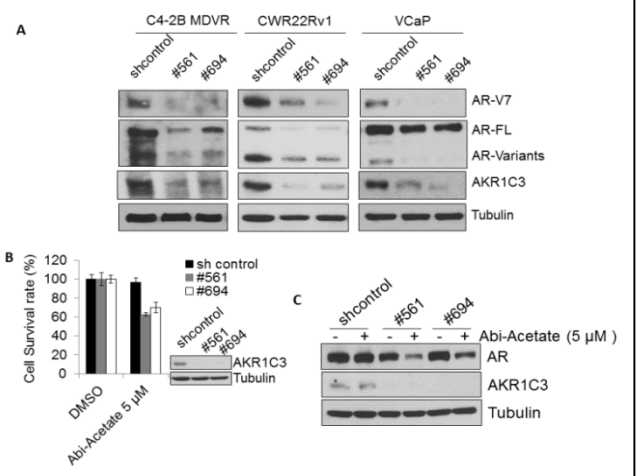

Figure 8. A. shRNA knockdown of AKR1C3 in C4-2B MDVR, CWR22Rv1 and VCaP cells. B. shRNA knockdown of AKR1C3 in C4-2B AbiR cells resensitized the Abi acetate treatments; and C. validation of the knockdown.

#649 both successfully reduced AKR1C3 and drastically decreased AR-V7 levels.in all three cell lines **(Figure 8A**). Concomitantly, AR full-length protein was also compromised in both C4-2B MDVR and CWR22Rv1 cells. Knocking down AKR1C3 in the AbiR cells resensitized them to Abi acetate treatments and decrease the full-length AR levels. (**Figures 8B and 8C**).

Orthotopic model of LNCaP-AKR1C3 tumor with Enza treatments (led by Dr. Evans' and assisted by Dr. Gao's Labs)

We next tested whether ARK1C3 overexpression would promote the aggressiveness and drug resistanced of PCa tumors in an orthtopic setting. Before conducting the animal study, we propagated LNCaP neo and AKR1C3 cells in CS medium over time and confirmed that LNCaP-AKR1C3 cells proliferated twice faster than the parental ones (**Figure 9A**). Two millions of LNCaP-AKR1C3 cells were mixed with matrigel and injected into the prostate of male SCID mice. When the serum PSA level reached 5-10 ng/ml, mice were surgically castrated. The animals were divided into two groups 2 weeks post castration to be treated with 25 mg/kg of Enza or buffer only (M-F, p.o). Tumor progression was continually monitored by serum PSA and mice were sacrificed after 3 weeks of treatments (**Figure 9B**). Tumors were harvested and compared. Throughout the course, LNCaP-AKR1C3 tumors continued to grow in castrated mice with increased serum PSA. Enza treatments did not prevent tumor progression; there was no difference between tumors from the control and treatment groups visually or by weight (**Figures 9C and 9D**). LC-MS measurement of the intracrine androgens in these tumors is underway.

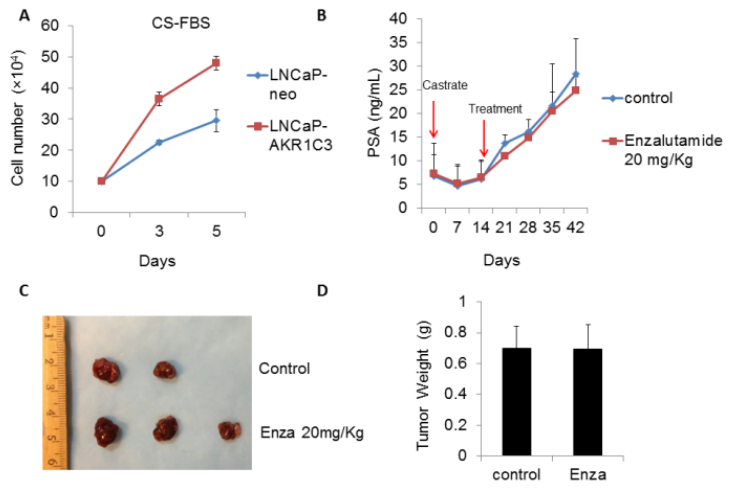

Figure 9. A. Growth curves of LNCaP neo and AKR1C3 cells in CS medium; B. serum PSA monitoring of tumor progression; C. representative tumor pictures and D. tumor weight of control and Enza treated groups.

We have shown that overexpression of AKR1C3 is responsible for the elevated intracrine androgen biosynthesis in prostate cancer cells. Up-regulation of AKR1C3 is correlated with anti-androgen resistance. We therefore sought to knock down AKR1C3 with specific siRNA and shRNA to confirm its role in androgen synthesis and drug resistance.

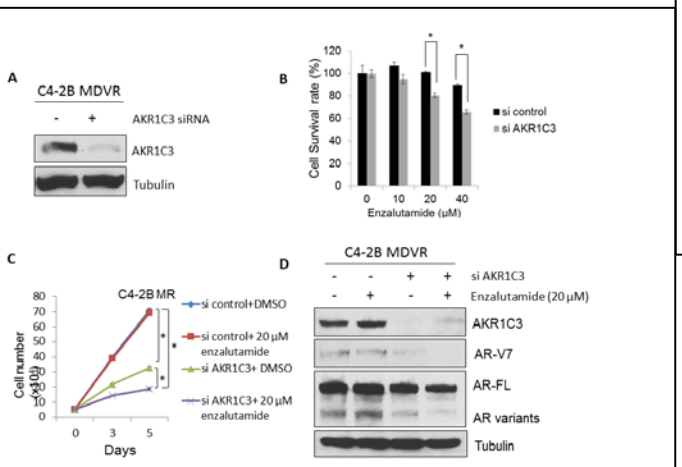

Figure 11 C4-2B MDVR cells were transfected with siAKR1C3 (A), treated with enza in a dose-response (B) and time-dependent (C)

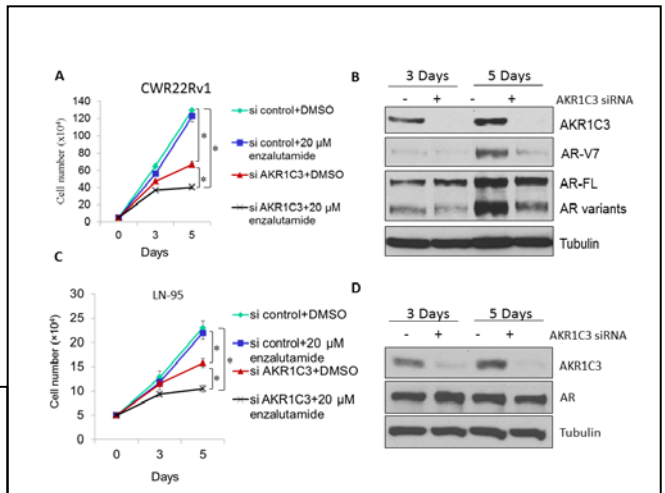

Figure 10 Growth response of CRW22Rv1 (A) and LN-95 (C) cells transfected with siAKR1C3 or control treated with enza. Western blots of CRW22Rv1 (B) and LN-95 (D) cells transfected

Determine whether blocking AKR1C3 expression inhibits intraprostatic androgen biosynthesis (led by Dr. Gao and assisted by Dr. Evans' labs) To demonstrate blockade of intracrine androgen synthesis through AKR1C3 down-regulation, we first need to use interference to knock down AKR1C3 either genetically or functionally.

Down regulation of AKR1C3 using siRNA in C4-2BMDVR and CWR22rv1 cells. We used two cell lines, CWR22Rv1 and LN-95 with high levels of AKR1C3 to test the effect of siRNA. These two cells are readily resistant to anti-androgen enzalutamide. Upon sampling 3 and 5 days post transfection with siAKR1C3, both CWR22Rv1 and LN-95 cells (**Figure 10**) showed satisfactory knockdown of AKR1C3. This knockdown caused inferior cell growth over 5 days in both cell lines and restored their sensitivity of cells to 20 μM enzalutamide (enza). AR variant 7 (AR-V7), the driver of enza-resistant in Rv1 cells was reduced along with AKR1C3 knockndown. The pool of AR variants also decreased. Protein levels of AR full length (AR-FL) in both cells remained unchanged. With the same token, C4-2B MDVR cells (**Figure 11**) were transfected with siAKR1C3 to knock down the molecule. This knockdown re-sensitizes C4-2B MDVR cells to enza treatment in a dose-response and time-dependent manner. AR variants, especially AR-V7, previously found to be enhanced in C4-2B MDVR cells were reduced to almost no detection upon the siRNA transfection. We also explored using shRNA against AKR1C3 to knock down the enzyme. Two shRNA's #561 and #694 were used to infect CWR22Rv1 and C4-2B MDVR cells. Knocking down of AKR1C3 re-sensitized these two castration resistant lines to enza treatment (**Figure 12**). In addition to its enzymatic activity in androgen synthesis, AKR1C3 has been suggested as an AR coactivator. We used shRNA knockdown to examine the influence of AKR1C3 on AR activity in C4-2B MDVR cells. Knockdown of AKR1C3 expression

significantly inhibited the expression of the AR target genes such as PSA and NKX3.1 (**Figure 13A, B**). To further understand how AKR1C3 modulates AR transcriptional activity, luciferase and ChIP assays were performed. Knockdown of AKR1C3 significantly inhibited PSA luciferase activity and

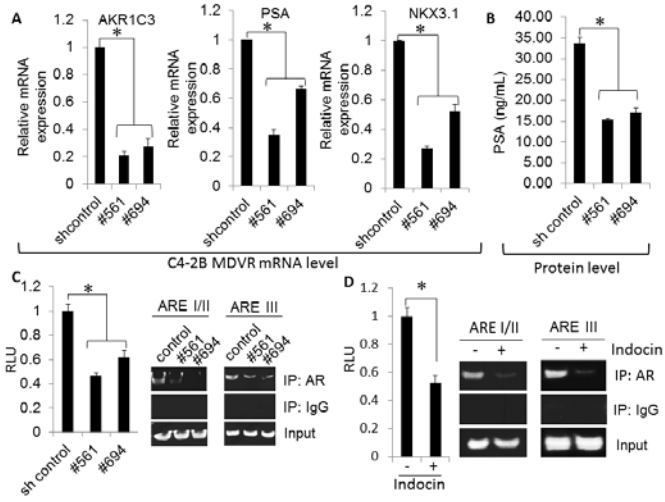

Figure 13 A. RT-qPCR of AKR1C3 and AR downstream genes PSA and NKX3.1 after shAKR1C3 transfection of C4-2B MDVR cells. B. ELISA measurement of PSA level after shAKR1C3 knockdown. PSA-Luc and ChIP assays of C4-2B MDVR cells infected with shAKR1C3 (C) or treated with Indocin (D).

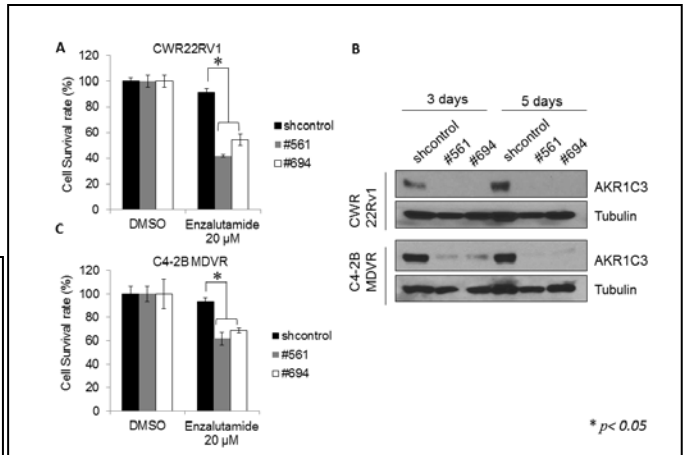

Figure 12 CWR22Rv1 (A) and C4-2B MDVR (C) cells were infected with shRNA's (#561 and #694) against AKR1C3 and treated with enza for cell survival assay. B. Knockdown of AKR1C3 were

reduced the recruitment of AR to the AREs (**Figure 13C**). The results were confirmed by use of the AKR1C3 enzyme inhibitor Indomethacin (Indocin). Treatment with Indocin significantly inhibited PSA luciferase activity and reduced the binding of AR to the AREs in C4-2B MDVR cells (**Figure 13D**).

Confirm that intracrine androgens are downregulated by AKR1C3 interference in C4-2B MDVR and CWR22rv1 cells. We attempted to use the siRNA or shRNA knockdown techniques to prepare cells void of AKR1C3 for intracellular steroid measurement. However, neither approaches warrant a stable system to allow collection of large mass of cells for the LC-MS measurement. After some failure, we resorted to use AKR1C3 inhibitor Indocin to perform the task. Fifty millions (5×10^7) of C4-2B MDVR and CWR22Rv1 cells treated with DMSO or 20 μM Indocin were harvested before maintained in serum- and phenol-red free medium for 3 days.

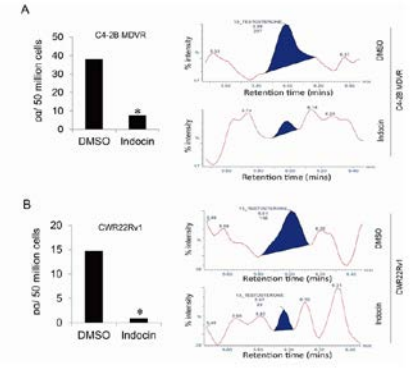

Metabolites (pg/50million cells)	C4-2B MDVR	C4-2B MDVR +Indocin	CWR22RV1	CWR22Rv1 +Indocin
Cholesterol	916.6	0.0	0.0	0.0
7-keto-25-OH cholesterol	37.3	0.0	0.0	0.0
Coprostanol-7,12-diol	49951.6	52995.9	78810.4	65048.4
27-OH-Cholesterol	195.3	1779.8	985.3	0.0
24-Hydroxycholesterol	1127.4	2016.7	3887.7	3917.2
5α,6α-epoxycholesterol	203.4	195.3	0.0	42.4
Cholesterol-3-SO4	29843.3	26536.9	2859.3	3945.5
Cholesterol-3-Glu	0.0	70.9	0.0	397.7
21-Hydroxypregnanolone	0.0	165.9	58.9	0.0
20α-Hydroxy-5α-pregnan-3-one	0.0	0.0	70.1	316.5
17α,20α-Dihydroxyprogesterone	149.0	119.1	216.7	84.0
Pregnelone	0.0	0.0	0.0	13.1
Progesterone	46.1	25.2	0.6	2.0
17-HYDROXYPROGESTERONE	3.0	0.0	2.4	2.8
Testosterone-GLUC	120.6	5.9	42.7	4.3
ANDROSTENEDIONE	0.0	0.0	0.0	15.8
TESTOSTERONE	38.1	7.7	14.8	0.0
Estrone	2.9	1.7	7.0	12.6
ESTRADIOL	70.0	104.1	6.4	14.3
2-OH ESTRONE	40.8	16.1	7.1	5.9
6-DEHYDROESTRADIOL	0.0	0.0	0.0	276.5
CORTEXONE	9.8	0.0	8.1	1.1
CORTICOSTERONE	0.0	0.0	81.3	34.4

Figure 14 Steroids by LC-MS measurement in C4-2B MDVR (A) and CWR22Rv1 (B) cells treated with 20 μM Indocin or DMSO. A. Testosterone; B. detailed lineups of various steroids detected in respective cells.

Steroids were extracted from cell pellets with 50% methanol and the supernatants were lyophilized followed by subsequent reconstitution to lower the total volume for LC-MS analysis. Both C4-2B MDVR and CWR22Rv1 cells expressed a significant higher level of testosterone than the Indocin treated counterparts (**Figure 14A, B**). Inhibition of AKR1C3 by Indocin drastically reduced or diminished the level of testosterone. Details of various steroids detected in response to Indocin treatment were shown in **Figure 14C**. These results echoed with the decreased AR binding to AREs and PSA- Luc activity in Indocin-treated C4-2B MDVR cells.

Examine the effects of inhibition of AKR1C3 to improve enzalutamide treatment in vivo tumor xenograft models (led by Dr. Evans' and assisted by Dr. Gao's Labs) To study how to target AKR1C3, it is more feasible to use the specific, small molecule inhibitor such as Indocin for in vivo studies. We tested two concentrations of Indocin, 10 and 20 μM, to treat C4-2B parental and MDVR cells in the presence or absence of enza (**Figure 15**). Indocin alone inhibits proliferation of C4-2B lines by around 20%. However, Indocin resensitizes MDVR cells to enza and reduces cell growth to the same level as the parental line. Clongenic assay also confirmed the result.

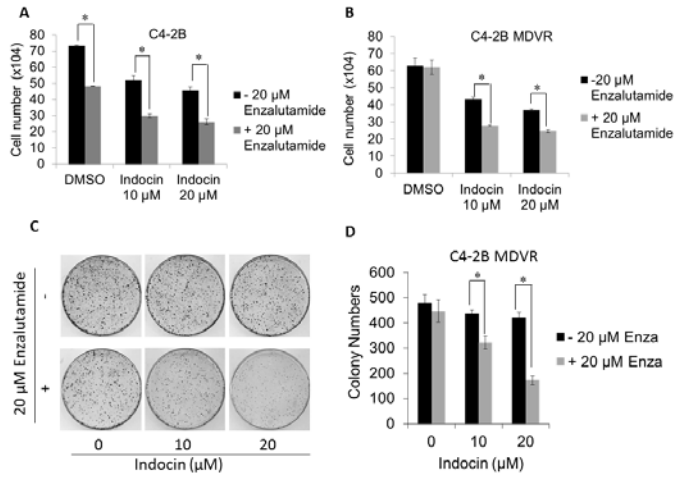

Figure 15 Growth inhibition of C4-2B parental (A) and MDVR (B) cells by indocin in combination with enza. Clongenic assays: C. Colony pictures of of C4-2B cells treated with Indocin and enza, and D. results

Effects of indomethacin to improve enzalutamide treatment in vivo tumor xenograft models. With the encouraging in vitro data of Indocin, we proceeded to the animal studies with the CWR22Rv1 xenograft model. Four millions of CWR22Rv1 cells were mixed with equal volume of matrigel and injected subcutaneously in to the flanks of male SCID mice. After tumor sizes reached 80 mm^3, mice were divided randomly into four groups and treated with enza (25 mg/kg, p.o), Indocin (3 mg/kg, p.o.), combination or control (vehicle only). Tumor progression was monitored by bi-weekly caliper measurement and animals were sacrificed after 3 weeks of treatment. Enza treatment only marginally reduced the tumor

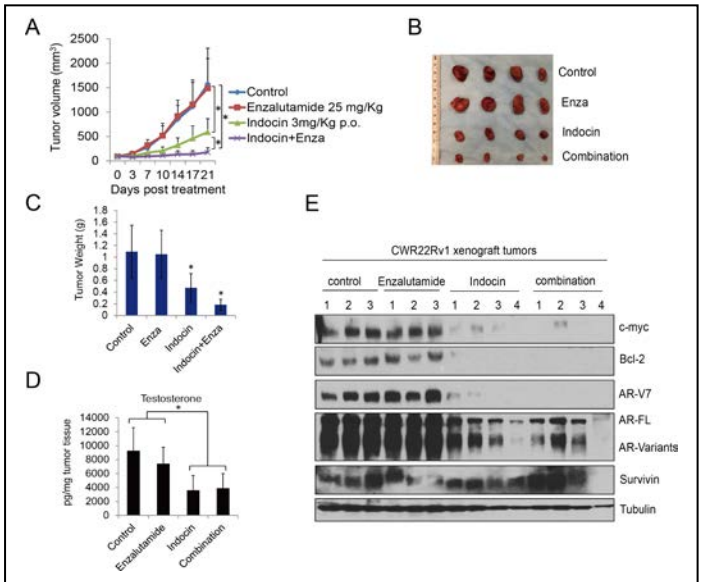

Figure 16 CWR22Rv1 xenograft model treated with control, enza, Indocin or combination. A. Tumor volume over time. B. Collected tumor pictures. C. Tumor weights. D. Testosterone level in tumor

growth. Indocin alone inhibits tumor growth significantly (**Figure 16**). Combination of Indocin and enza further blocks tumor development. Intratumoral testosterone measurement by LC-MS shows that Indocin effectively maintains testosterone at a significant lower level than that in control and enza groups. At a closer look at the tumor samples from each treatment groups by Western blots, AR-V7 levels are almost completely diminished in the two Indocin groups, suggesting a direct modulation of AR-V7 through targeting AKR1C3. When blotted with antibody against the N-terminus of AR, levels of both AR full-length and variants are greatly reduced by Indocin treatment as well.

With the same principle, we looked at the effect of combination use of Indocin with the other FDA approved CYP17A1 inhibitor abiraterone (abi). Inhibition of CWR22Rv1 cell proliferation by abi Indocin alone or in combination (**Figure 17**), lines up in an orderly pattern, from the least to the most. Extent of colony formation after drug treatments confirms the trend. We then performed in vivo study with the CWR22Rv1 and SCID mice model using abi in place of enza for drug treatment. The tumor growth curve is similar to the previous study, with abi demonstrating no effect in retarding tumors and yet combination with Indocin yielding a tumoristatic curve. Again, Indocin alone may reduce tumor growth but the combination of abi and Indocin completely prevent tumor growth, which is validated by Ki67 staining.

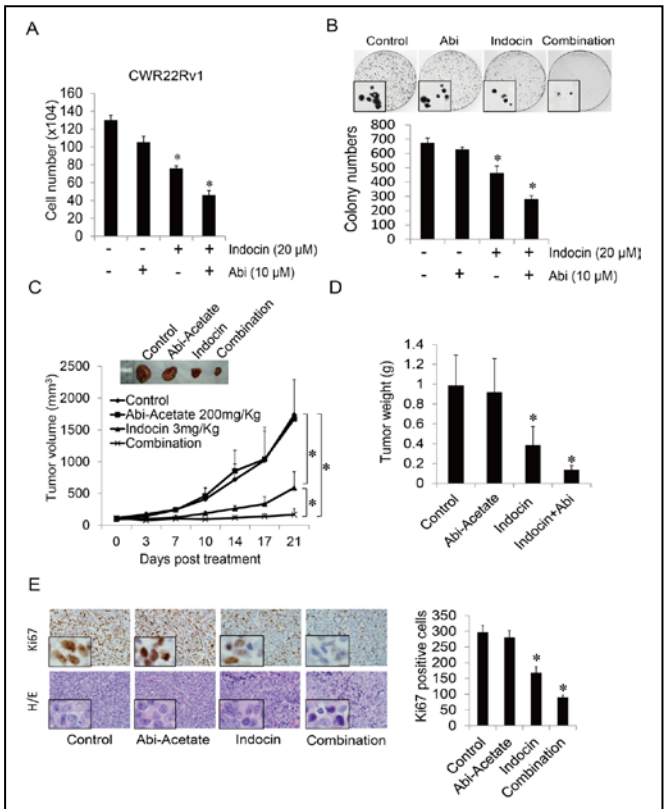

Figure 17 CWR22Rv1 cell and xenograft models treated with control, abi, Indocin or combination. A. Cell growth inhibition by single or double agents. B. Clongenic assays with colony pictures and counts vs. treatments. C. Tumor volume over time with representative tumor pictures. D. Tumor weights. E.

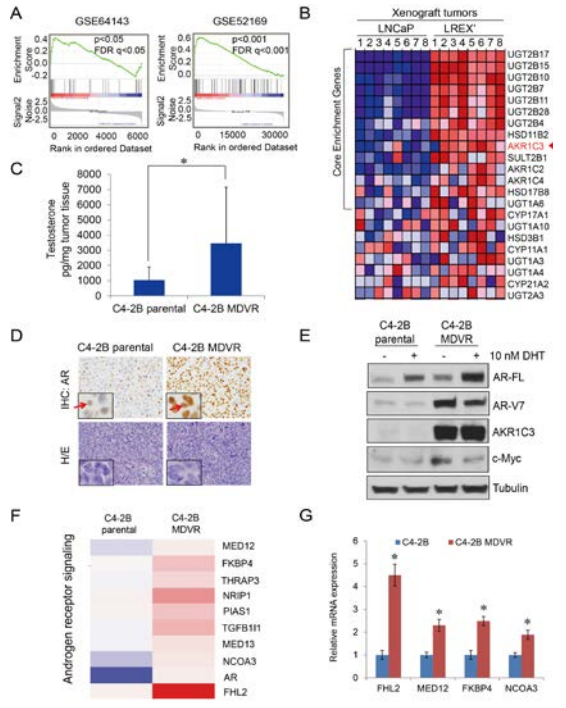

Figure 18 Comparisons between C4-2B parental vs. MDVR cells or tumors (A) steroid hormone biosynthetic pathway (B) steroidogenesis in LNCaP vs. LREX' xenograft tumors (C) Testosterone levels (D) AR IHC staining (E) WB of DHT stimulation after CS medium (F) androgen receptor signaling genes.

We examined C4-2B MDVR (enzalutamide resistant) cells closer and found that in addition to AKR1C3, a

whole array of steroid biosynthetic genes were also upregulated (**Fig. 18A, B**). C4-2B MDVR xenograft tumors expressed significantly higher testosterone levels compared to C4-2B parental xenograft tumors (**Figure 18C**). IHC staining of AR in C4-2B MDVR xenografts was predominately in the nucleus compared to C4-2B parental tumors (**Figure 18D**). Addition of DHT into C4-2B cells maintained in androgen-deprived medium stimulated AR/AR-V7 protein levels and its signaling pathways with upregulation of co-activators (**Figures 18-G**)

AKR1C3 binds with AR-V7 and induces AR/AR-V7 protein overexpression (led by Dr. Gao and assisted by Dr. Evans' labs)

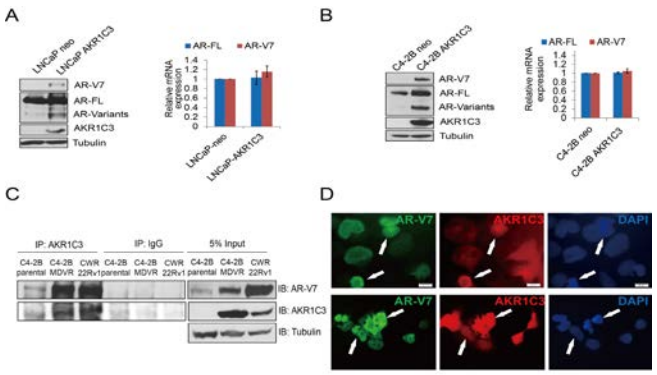

Figure 19 Effect of AKR1C3 overexpression (A) LNCaP (B) C4-2B cells (C) MDVR and Rv1 cells with AKR1C3 co-IP (D) dual IF stainingin MDVR and Rv1 cels.

Overexpression of AKR1C3 in LNCaP and C4-2B cells enhanced AR-V7 protein expression; full length AR (AR-FL) was also significantly in C4-2B-ARK1C3 cells (**Figures 19A, B**). However, no significant difference in the mRNA levels of AR-FL and AR-V7 in these cells. This induction might be due to the binding of AKR1C3 to AR-V7 demonstrated by both co-immunoprecipitation and dual immunofluorescence staining (**Figures 19C, D**). AKR1C3 overexpression also enabled LNCaP cells to grow in CS-FBS condition (**Figure 20A**). These cells once grown in to tumors, responded to castration with slight regression and delay in tumor volume increase for two weeks. Once relapse, tumor progression was not affected by daily treatment of enzalutamide (20 mg/kg), almost identical to that in the control group. Western blot analysis showed an induction of AR-V7 post castration, suggesting enzalutamide resistance in castrated LNCaP-AKR1C3 tumors (**Figures 20B-D**). In parallel, knocking down AR-V7 in LNCaP-AKR1C3 and C4-2B-AKR1C3 cells slightly decreased cell proliferation and combination with enzalutamide significantly suppressed cell growth (**Figure 20E, F**).

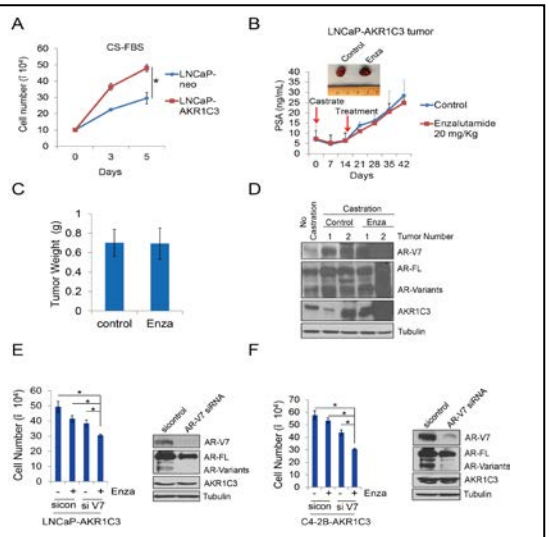

Figure 20 (A) LNCaP neo and AKR1C3 cells growth curves in CS medium (B) LNCaP AKR1C3 tumor growth after castration and treatment with or without enzalutamide (C) tumor weights (D) WB analysis of tumors. AR-V7 knockdown effect on cell growth and protein (E) LNCaP-AKR1C3 (F) C4-2B-AKR1C3

AKR1C3 controls AR and AR-V7 protein stabilization in resistant prostate cancer cells

We reasoned that the underlying mechanism of AKR1C3 mediated AR-V7 upregulation may be at the protein level since there was no significant change in the AR-FL or AR-V7 mRNA levels. AR/AR-V7 protein stability was determined in C4-2B-neo and C4-2B-AKR1C3 cells. In C4-2B neo cells, AR-FL protein levels were apparently decreased when cells were maintained in the presence of cycloheximide (CHX), the inhibitor for protein synthesis. When translation elongation was inhibited by CHX, no new protein was synthesized while the old one continued to be turned over. AR level dropped to 50% within 4 hours after cycloheximide addition (**Figure 21A**). AR-V7 was scant in the neo cells and diminished within 2 hours from the beginning of incubation. In contrast, AR protein level was steadily maintained throughout 8 hours of test period due to the high level of AKR1C3 in C4-2B-AKR1C3 cells. Both the levels of AR-V7 and variants were near constant as well. Knockdown of AKR1C3 in cells with high level of AKR1C3 such as CWR22Rv1 (**Figure 21B**) and C4-2B MDVR (**Figure 21C**) cells reverted AR/AR-7 protein stability to the state as that in neo cells. Inhibition of AKR1C3 with the potent inhibitor indomethacin suppressed AR and AR variants expression in C4-2B MDVR cells (**Fig.21D**). Proteasome inhibitor MG132 maintained AR/AR-V7 protein expression in C4-2B MDVR cells treated with indomethacin (**Fig.21E**). Immunoprecipitation of AR-V7 with its antibody in C4-2B MDVR cells showed that the variant was heavily ubiquitinated upon indomethacin treatment, suggesting AKR1C3 protects AR-V7 from ubiquitination degradation in the enza resistant cells (**Figure 21F**).

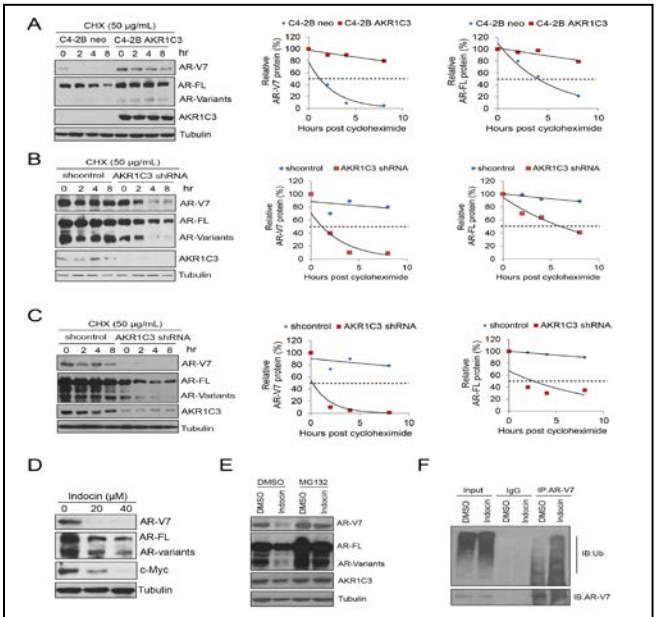

Figure 21 AR-FL/AR-V7 protein stability (A) C4-2B neo vs. AKR1C3 cells (B) knockdown of AKR1C3 in CWR22Rv1 cells (C) in C4-2B MDVR cells (D) treatment with indomethacin in MDVR cells (E) with MG132 inhibition on the effect of Indocin treatment (F) ubiquitination of AR-V7 by co-IP.

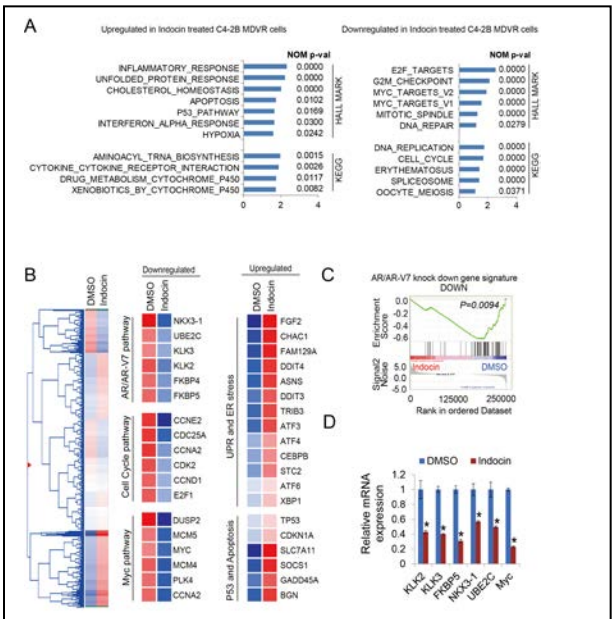

Figure 22 RNA-seq analysis of C4-2B MDVR cells treated with indomethacin (A) GSEA showed up and down-regulated pathways (B) heatmap plots showed individual genes (C) significant downregulation of AR/AR-v7 pathway by indomethacin (D) qRT-PCR validation of representative genes .

Inhibition of AKR1C3 with indomethacin disrupts gene programs and suppresses AR/AR-V7 signaling in resistant cells

We use RNA-seq analysis to scrutinize the effect of indomethacin. By GSEA, the top pathways upregulated in indomethacin treated C4-2B MDVR cells are

unfolded protein response (UPR), p53 signaling, apoptosis and hypoxia pathways; and downregulated, E2F targets, cell cycle and Myc targets (**Figure 22A**). Heatmap plots (**Figure 22B**) reveal the individual genes, especially those downregulated in AR/AR-V7 (such as KLK2, KLK3, FKBP5, Nkx3-1 and Ube2C), cell cycle and Myc pathways. On the other hand, indomethacin upregulated an array of genes in UPR and ER stress pathway, as well as those responsible for P53 and apoptosis pathway. The inhibitory effect of indomethacin on AR/AR-V7 pathway is significant (**Figure 22C**). This was validated by qRT-PCR, expression of AR/AR-V7 downstream genes and Myc were significantly decreased by indomethacin (**Figure 22D**).

Orally administered of indomethacin enhances enzalutamide treatment through AKR1C3/AR-V7 inhibition (led by Dr. Evans' and assisted by Dr. Gao's Labs)

Previous data suggested indomethacin enhanced enzalutamide treatment when administered through intraperitoneal (i.p.) injection. To further identify the potential activity of indomethacin *in vivo*, we determined its tumor inhibition effects though oral administration. As shown in **Fig.23A-C**, CWR22Rv1 tumors were completely resistant to enzalutamide treatment, orally administered indomethacin significantly reduced tumor growth, and indomethacin combined with enzalutamide treatment further suppressed tumor growth. However, all treatment did not affect the mice body weight (**Fig.23D**). We also determined the intratumoral testosterone level of each group, as shown in Fig.6E, enzalutamide slightly decreased the testosterone level, however, indomethacin and indomethacin plus enzalutamide treatment group significantly decreased the tumor testosterone level. We also extracted tumor proteins and found that indomethacin alone and the combination treatment groups significantly decreased AR/AR-V7, c-Myc and Bcl-2 expression in these tumors. These results suggest that targeting AKR1C3 with small molecule indomethacin enhances enzalutamide treatment *in vivo* through suppressing both intratumoral testosterone and AR-V7 expression.

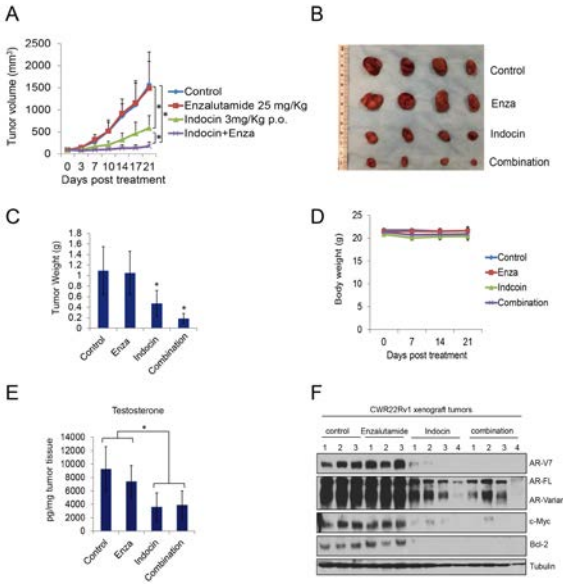

Figure 23 CWR22Rv1 xenograft model treated with control, enza, Indocin or combination. (A) Tumor growth curve (B) Representative tumor pictures (C) Tumor weights (D) Mouse body weight in each group (E) Intratumoral testosterone (F) Western blots of AR-FL and AR-V7 from all treatment groups.

Correlation of hnRNPA1 with AKR1C3 in AR-V7 upregulation (led by Dr. Gao and assisted by Dr. Evans' labs)

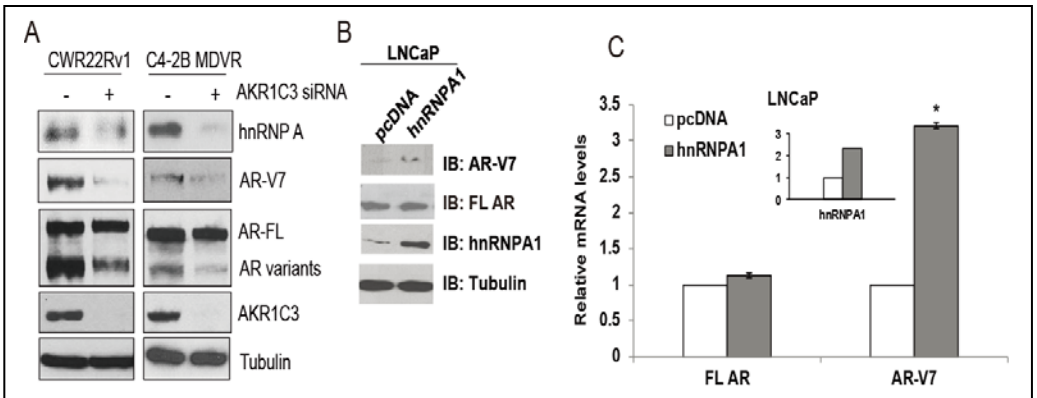

Figure 24 (A) Knockdown of AKR1C3 in CWR22Rv1 and C4-2B MDVR cells decreased hnRNPA1 expression. Overexpression of hnRNPA1 in LNCaP cells upregulated AR-V7 in (B) WB and (C) RT-qPCR

One possible mechanism for the increase in AR variants expression could be changes in expression of factors such as RNA binding proteins that regulate AR slicing patterns. Alternative splicing leads to the production of multiple mRNAs from a single gene. Our preliminary data suggest that AKR1C3 regulates ARv7 expression. Knock down of AKR1C3 expression reduced ARv7 expression in both CWR22rv1 and C4-2BMDVR cells (**Figure 24A**), which correlated with down regulation of hnRNPA expression. In addition, overexpression of HnRNPA1 in LNCaP cells increased ARv7 protein (**Figure 24B)** and mRNA expression (**Figure 24C**). These data suggest that AKR1C3 increases ARv7 expression through upregulation of HnRNPA.

Treatment of Qucertin decreases and AR-V7 expression through regulating hnRNP

Qucertin in one of the components of fruit and seed extracts used in food supplements. Treatment of C4-2B MDVR cells with Qucertin over various time downregulated expression of hnRNPA1, AR-V7 and AR-FL both at the mRNA and protein levels (**Figure 25**).

In summary, we examined closer on the underlying mechanisms how AKR1C3 regulates the upregulation of AR/AR-V7 expression in enzalutamide resistant prostate cancer cell models. Changes in gene profiling supported AR/AR-V7 downstream gene signaling. And AKR1C3 functions through binding to AR/AR-V7 and protecting them from ubiquitination degradation. AKR1C3 inhibitor indomethacin inhibited tumor growth of a CRPC line, CWR22Rv1; combination use of indomethacin and enzalutamide completed blocked tumor progression. Targeting hnRNPA1, an RNA splicing enzyme, with food supplement Qucertin also downregulated AR/AR-V7 in enzalutamide resistant cells. Overall, we show therapeutic potential of using AKR1C3 inhibitor to treat anti-androgen resistant prostate cancer patients.

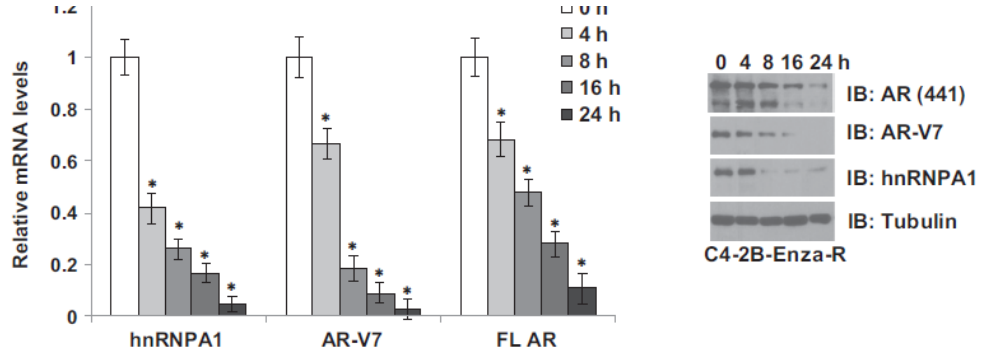

Figure 25 Treatment of Qucertin in C4-2B MDVR cells decreased hnRNPA1, AR-V7 and AF-FL at mRNA and protein levels.

AKR1C3/AR-V7 axis confers cross-resistance to apalutamide and darolutamide

C4-2B MDVR cells with elevated levels of AR-V7 and AKR1C3 display cross resistance to two new anti-androgen drugs, Apalutamide and Darolutamide. To test if the AKR1C3/AR-V7 axis confers cross-resistance to apalutamide and darolutamide, we determined if knockdown of AKR1C3 re-sensitizes the resistant cells to apalutamide and darolutamide. As shown in **Fig.26A**, knockdown of AKR1C3 by lenti-AKR1C3 shRNA inhibited cell growth. AKR1C3 knockdown combined with apalutamide/darolutamide further reduced cell number compared to the control group. We furthed confirmed that knockdown of AKR1C3 significantly down-regulated AR, AR-V7, and c-Myc expression in C4-2B MDVR cells **(Fig.26B)**. To further confirm AKR1C3 is involved in apalutamide and darolutamide resistance, we used C4-2B-AKR1C3 cells to test whether exogenous expression of AKR1C3 induces apalutamide or

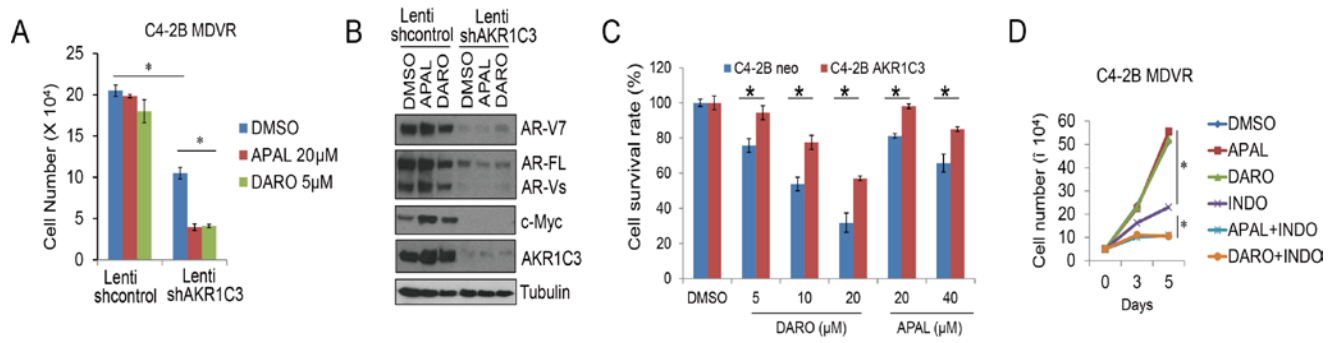

Figure 26. AKR1C3 confers apalutamide and darolutamide resistance through AR-V7 regulation. A-B. C4-2B MDVR cells were infected with lenti-control shRNA or lenti-AKR1C3 shRNA and then treated with 20 μM apalutamide or 5 μM darolutamide and cell numbers were determined after 5 days. Whole cell lysates were collected and subjected to western blot. C. C4-2B neo or C4-2B AKR1C3 cells were treated with different concentrations of apalutamide or darolutamide for 3 days, total cell numbers were counted and cell survival rate (%) was calculated. D. C4-2B MDVR cells were treated with 20 μM apalutamide or 5 μM darolutamide or 20 μM indomethacin, alone or in combination, total cell numbers were determined on 3 and 5 days. APAL: apalutamide, DARO: darolutamide. INDO: indomethacin * $p<0.05$.

darolutamide resistance. As shown in **Fig.26C**, C4-2B-AKR1C3 cells exhibited greater resistance to apalutamide and darolutamide than C4-2B-neo cells. Finally, AKR1C3 inhibitor indomethacin significantly enhanced both apalutamide and darolutamide treatment in C4-2B MDVR cells in a time dependent manner **(Fig.26D)**. At 5 days treatment, the coefficient of drug interaction (CDI) of indomethacin with apalutamide and darolutamide combination treatment were 0.56 and 0.64 respectively, suggesting synergistic interactions (CDI<1). In light of these results, our data indicated that the AKR1C3/AR-V7 axis is one of the major mechanisms conferring apalutamide/darolutamide cross-resistance to enzalutamide in advanced prostate cancer.

Chronic apalutamide treatment in C4-2B cells upregulates the steroid biosynthesis pathway

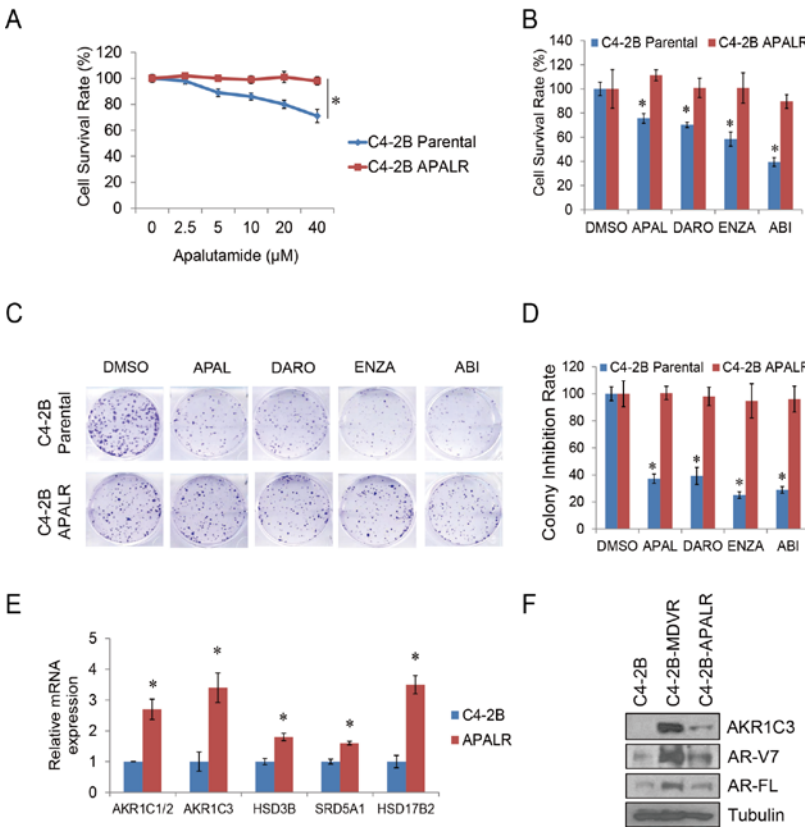

Figure 27. Chronic apalutamide treatment in C4-2B cells activates the steroid biosynthesis pathway through AKR1C3 upregulation. A. C4-2B parental and C4-2B APALR cells were treated with different concentration of apalutamide for 3 days, total cell numbers were determined and cell survival rate was calculated. B. C4-2B parental and C4-2B APALR cells were treated with 20 μM apalutamide, 5 μM darolutamide, 20 μM enzalutamide or 10 μM abiraterone and cell numbers were determined after 3 days. C-D. The clonogenic ability of C4-2B parental and C4-2B APALR cells treated with 20 μM apalutamide, 5 μM darolutamide, 20 μM enzalutamide or 10 μM abiraterone was analyzed. E. The genes involved in steroid hormone biosynthesis pathway were determined by qRT-PCR. F. Whole cell lysates were collected from C4-2B parental, C4-2B MDVR and C4-2B ARNR cells and subjected to western blot. Enza: enzalutamide, APAL: apalutamide, Abi: abiraterone acetate, DARO: darolutamide. * $p<0.05$

Apalutamide is a new next-generation anti-androgen with a molecular structure very similar to enzalutamide. To investigate apalutamide resistance, we have successfully generated a C4-2B apalutamide resistant cell line (C4-2B APALR). As shown in **Fig.27A**, C4-2B parental cells were seneitive to apalutamide treatment in a dose dependent manner; however, C4-2B APALR cells were resistant. To test if cross-resistance exists between apalutamide and other androgen signal-targeting agents in this cell model, C4-2B APALR cells were treated with apalutamide, darolutamide, enzalutamide and abiraterone. Both cell growth **(Fig.27B)** and colony formation assays **(Fig.27C-D)** confirmed that C4-2B APALR cells exhibited robust resistance not only to apalutamide but also to darolutamide, enzalutamide and abiraterone. We then examine the transcriptional alterations of steroid hormone biosynthesis related genes in C4-2B APALR cells compared to the parental ones. The steroid hormone biosynthesis related genes were significantly upregulated in C4-2B APALR cells compared to C4-2B parental cells **(Fig.27E)**. Results from western blot indicated that the protein levels of both AKR1C3 and AR-V7 are overexpressed in C4-2B APALR cells . However, these levels were lower than those in C4-2B MDVR cells (**Fig.27F**). These results strongly imply that the AKR1C3/AR-V7 axis is critical in conferring cross-resistance between apalutamide and other anti-androgens.

Targeting AKR1C3 resensitize apalutamide resistant cells to apalutamide and enzalutamide

To confirm the contribution of the AKR1C3/AR-V7 axis in cross-resistance between enzalutamide and apalutamide, C4-2B APALR cells were treated with enzalutamide or apalutamide with or without the knockdown of AKR1C3 by lenti-AKR1C3 shRNA **(Fig.28A)**. Growth of C4-2B APALR cells was largely inhibited by AKR1C3 knockdown. AKR1C3 knockdown in combination with enzalutamide/apalutamide treatment further reduced cell growth. The knockdown of AKR1C3 was accompanied with reduced expression levels of AR-FL, AR-V7 and c-Myc **(Fig.28B)**, which is consistent with what is observed in C4-2B MDVR cells. Finally, C4-2B APALR cells were treated with the AKR1C3 inhibitor indomethacin or apalutamide, alone and in combination. Indomethacin effectively resensitized C4-2B APALR cells to apalutamide treatment **(Fig28C),** the coefficient of drug interaction (CDI) of 40 μM apalutamide with 20 μM indomethacin or 40 μM indomethacin combination treatment were 0.61 and 0.63 respectively, suggesting drug synergism (CDI<1). The results were confirmed by clonogenic assay. 40 μM apalutamide has no effects on colony formation in C4-2B APALR cells, single indomethacin treatment reduced the colony formation and combination treatment significantly suppressed colony size and numbers **(Fig28D-E)**. Collectively, our data suggest that targeting AKR1C3 in apalutamide resistant cells could efficiently reverse cross- resistance between apalutamide and enzalutamide.

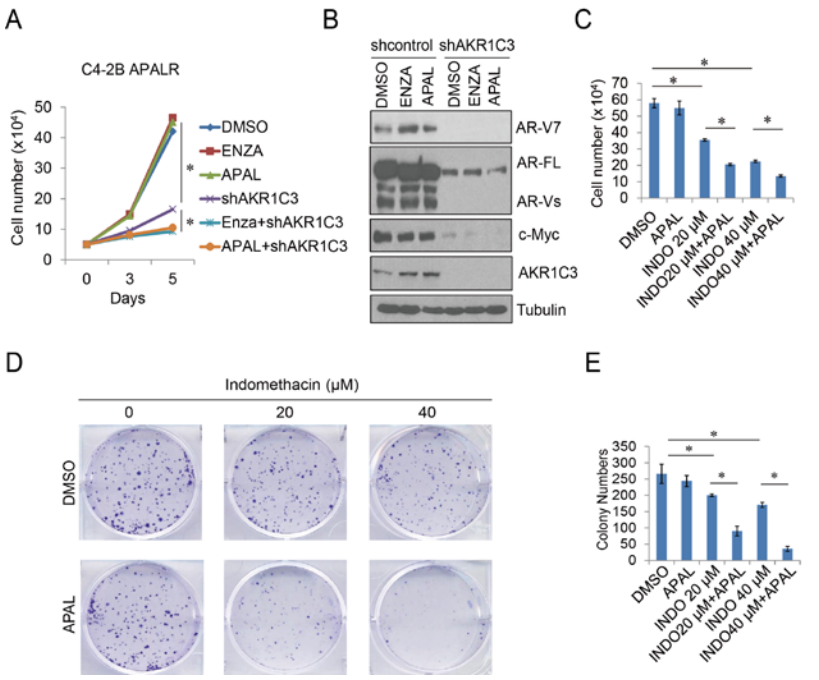

Figure 28. Targeting AKR1C3 resensitizes apalutamide resistant cells to apalutamide and enzalutamide. A. C4-2B APALR cells were treated with 20 μM enzalutamide, 20 μM apalutamide or infected with lenti-AKR1C3 shRNA, alone or in combination. Total cell numbers were determined on 3 and 5 days. B. C4-2B APALR cells were infected with lenti-control shRNA or lenti-AKR1C3 shRNA and then treated with 20 μM enzalutamide or 20 μM apalutamide. After 5 days, whole cell lysates were collected and subjected to western blot. C. C4-2B APALR cells treated with 0, 20, 40 μM indomethacin with or without 20 μM apalutamide and cell numbers were determined after 5 days. D-E. The clonogenic ability of C4-2B ARNR cells treated with 0, 20, 40 μM indomethacin with or without 20 μM apalutamide was analyzed. APAL: apalutamide, ENZA: enzalutamide. INDO: indomethacin * $p<0.05$.

In summary, we have accomplished all the tasks with teamwork. We have delineated the mechanisms through which AKR1C3 mediates resistance to enzalutamide. We generated tet-inducible LNCaP/TR/AKR1C3 cells. We with the help of our collaborator performed the measurement of intracrine androgens in AKR1C3 overexpressing cells. We also used another drug-resistant line, C4-2B AbiR cells to confirm the important role of AKR1C3 in drug resistance possibly through up-regulating AR-V7.

We used siRNA, shRNA specific to AKR1C3 and a small molecule inhibitor Indocin to target AKR1C3. At cellular level, we demonstrated that knockdown AKR1C3 may 1. Restore sensitivity to anti-androgen drugs such as enzalutamide and abiraterone. 2. Reduce AR-V7 level. 3. Inhibit AR transactivation activity. 4. Abate intratumoral androgen synthesis. Using Indocin to target AKR1C3 in vivo is efficient in reducing tumor sizes and further successful in blocking tumor growth when combined with either enzalutamide or abiraterone. AKR1C3 controls the protein stability of AR/AR-V7 in anti-androgen resistant prostate cancer cells. In addition, it may regulate the expression of the RNA splicing enzyme hnRNPA1, which contributes to the level of AR-V7 and this action may be inhibited by Qucertin. The AKR1C3/AR-V7 axis is the main driving force of cross resitance among anti-androgens such as enzalutamide and apalutamide in advance prostate cancer.

4. IMPACT

Our study discovered a novel mechanism by which AKR1C3 induces AR-V7 protein stabilization via activation of the ubiquitin proteasome pathway system activation. We show that AKR1C3 reprograms AR/AR-V7 signaling in enzalutamide resistant cells. AKR1C3 induces AR-V7 overexpression and stabilizes AR-V7 protein in resistant cells through alteration of the ubiquitin proteasome system. Targeting AKR1C3 by indomethacin activates UPR and p53 pathways but suppresses AR/AR-V7 signaling. Orally administrated indomethacin significantly enhances enzalutamide treatment through AKR1C3/AR-V7 signaling suppression. Additionaly, we also found out that AKR1C3 regulated RNA splicing factor hnRNPA1 expression. HnRNPA1 regulated AR-V7 expression in resistant cells. Additionally, we found apalutamide and darolutamide share similar resistant mechanisms with enzalutamide and abiraterone. The AKR1C3/AR-V7 complex confers cross-resistance to second generation AR-targeted therapies in advanced prostate cancer. Our results highlight the role of AKR1C3/AR-V7 complex in enzalutamide and abiraterone resistance.

5. CHANGES/PROBLEMS

Nothing to report.

6. PRODUCTS:

Publications, conference papers, and presentations

1. Zhao J, Ning S, Lou W, Yang JC, Armstrong CM, Lombard AP, D'Abronzo LS, Evans CP, Gao AC, Liu C. Cross-resistance Among Next Generation Anti-Androgen Drugs Through the AKR1C3/AR-V7 Axis in Advanced Prostate Cancer. Mol Cancer Ther. 2020 19(8):1708-1718

2. Liu C, Yang JC, Armstrong CM, Lou W, Liu L, Qiu X, Zou B, Lombard AP, D'Abronzo LS, Evans CP, Gao AC. AKR1C3 promotes AR-V7 protein stabilization and confers resistance to AR-targeted therapies in advanced prostate cancer. Mol Cancer Ther. 2019 18(10):1875-1886
3. C Pan, P Lara, CP Evans, M Parikh, R de Vere White, M Dall'era, Liu C. A phase Ib/II trial of indomethacin and enzalutamide to treat castration-resistant prostate cancer (CRPC). 2018.Journal of Clinical Oncology 36 (6_suppl), TPS394-TPS394
4. Liu C, W Lou, C Pan, P Lara, C Evans, M Parikh, R deVere White. Combination of indomethacin and enzalutamide to treat castration-resistant prostate cancer 2018. The Journal of Urology 199 (4), e694
5. Liu C, Armstrong CM, Lou W, Lombard A, Evans CP, Gao AC. Inhibition of AKR1C3 Activation Overcomes Resistance to Abiraterone in Advanced Prostate Cancer. Mol Cancer Ther, 2017,16(1): 35-44.

7. PARTICIPANTS & OTHER COLLABORATING ORGANIZATIONS

(1) Allen Gao, MD PhD (PI) No change

(2) Christopher P. Evans MD (Co-PI) No Change

Name	*Chengfei Liu, MD PhD*
Project Role	*Research Associate*
Researcher Identifier (e.g. ORCID ID):	694392333
Nearest person month worked:	3
Contribution to Project:	*No change*
Funding Support:	N/A
Name:	*Joy C. Yang, PhD*
Project Role:	*Project Scientist*
Researcher Identifier (e.g. ORCID ID):	663002459

Nearest person month worked:	12
Contribution to Project:	*No change*
Funding Support:	*N/A*

Has there been a change in the active other support of the PD/PI(s) or senior/key personnel since the last reporting period?

N/A

8. SPECIAL REPORTING REQUIREMENTS

Nothing to report

9. APPENDICES:

N/A